Study of Tyre Pyrolysis Oil Model Compound Structure on Carbon Nano-material Production

Yeshui Zhang[*1,2,3], Hualun Zhu[4], Ruike Zhang[5], Lu Yu[6], Ziqi Liu[7], Paul R. Shearing[1], Dan J.L. Brett[1], Paul T. Williams[*2]

[1] Electrochemical Innovation Lab (EIL), Department of Chemical Engineering, University College London, London, WC1E 7JE UK
[2] Energy Research Institute, School of Chemical and Process Engineering, University of Leeds, Leeds, LS2 9JT UK
[3] School of Engineering, University of Aberdeen, Aberdeen, AB24 3UE, UK
[4] Department of Chemical Engineering, Imperial College London, London, SW7 2AZ UK
[5] Nanyang Junhao Chemical.co.Ltd., Anpeng chemical industry zone, Tongbai County, Nanyang City, Henan Province, 473000, P.R. China
[6] Bureau of Ecology and Environment in Shashi District, Jingzhou, 434100, P.R. China
[7] School of Materials Science and Engineering, Jilin University, Jilin, 130015, P.R. China
*Correspondence: yeshui.zhang@ucl.ac.uk
                 p.t.williams@leeds.ac.uk

Abstract:

The pyrolysis-catalysis process of waste tyres has been reported to produce high value carbon nano-materials. Tyre pyrolysis oils contain a wide range of aliphatic and aromatic compounds. To further investigate the production of carbon nano-materials from waste tyres, model compounds have been investigated with a 10 wt.% Ni/Al_2O_3 catalyst to determine their influence on the production of carbon nano-materials. The compounds (hexadecane, decane, styrene, naphthalene and phenanthrene) were chosen to represent typical aliphatic and aromatic compounds detected in tyre pyrolysis oils. It has been found that the aromatic compounds dominated solid nano-carbon production compared with aliphatic compounds, especially for the production of highly graphitic filamentous carbon. The filamentous carbon produced from aliphatic compounds was in the range of 27.06 to 77.97 mg g^{-1} $_\text{of feedstock equivalent carbon}$ and the filamentous carbon produced from aromatic compounds ranged from 104.53 to 174.19 mg g^{-1} $_\text{of feedstock equivalent carbon}$. The filamentous carbon was further characterized by thermogravimetric analysis, electron microscopy and Raman spectroscopy, which confirmed that the filamentous carbon was composed of both hollow carbon nano-tubes and solid carbon nano-filaments. The quality of the produced filamentous carbon was shown by Raman spectroscopy analysis to be very similar to commercial filamentous carbon.

Keywords: Tyre oil, model compound, pyrolysis, catalysis; CNTs

Introduction

Carbon nano-materials such as carbon nanotubes (CNTs), solid carbon nano-filaments and hollow carbon nano-spheres have attracted much research interest because of their unique

physical and chemical properties.[1] Methods used for the production of carbon nano-materials include the chemical vapour deposition (CVD) process where pure hydrocarbons such as methane, ethene, acetylene or ethanol deposit on a solid substrate/catalyst.[2-5] In recent years, there has been research into the production of carbon nano-materials from alternative feedstocks, such as waste tyres,[6-9] wastes plastics,[10-12] crude glycerol[13] and biomass.[14-15] For example, waste tyres as the carbon source have been used to produce CNTs and nano-filaments. Due to the substantial carbon and hydrogen contents in waste tyre,[16] so the recovery of tyres has been investigated by many groups.[16-17] Recent work[17-21] showed that under optimum conditions, CNTs were formed during pyrolysis catalysis of waste tyres. Yang et al.[22] successfully produced CNTs by CVD method over a cobalt-based catalyst from waste tyres. This indicated waste tyres have great potential to be the carbon precursors for CNT production. Murr et al.[23] studied a novel electric arc discharge method to synthesis multi-walled carbon nanotubes (MWCNTs) from tyre . Poyraz et al.[24] synthesised CNTs from devulcanized tyre particles by using the short-term microwave irradiation which was firstly carried out in a microwave within 4 minutes.

The yield and structure of carbon nano-materials are closely relate to the chemical structure of the precursor hydrocarbon compounds. Tyre pyrolysis oil is a very complex tar composed of mainly aliphatic and aromatic compounds and to a lesser extent, heteroatom and polar compounds.[25] Aliphatic compounds as a chemical class fraction have been reported at more than 50 wt.% and aromatic fractions of more than 66 wt.%, but the proportions of aliphatic to aromatic fractions vary greatly due to pyrolysis process conditions. Typical identified aromatic hydrocarbons in tyre pyrolysis oils include, benzene, toluene, xylenes, styrene, limonene, indene, alkylated benzenes, alkylated indenes etc. Polycyclic aromatic hydrocarbon identified include 2-ring naphthalene and biphenyl, 3-ring phenanthrenes and anthracene, 4-ring pyrene and chrysene and 5-ring benzopyrenes and alkylated derivatives.[25] Identified aliphatic compounds include alkanes from C_{10} - C_{35} and alkenes from C_6 - C_9. In addition to the higher molecular weight hydrocarbons, the product gases from tyre pyrolysis will also pass into the second stage catalytic reactor and become involved in production of carbon nano-materials, such gases include, CH_4, C_2H_6, C_2H_4, C_3H_8, C_3H_6, C_4H_{10}, C_4H_8 and C_4H_6.

Our previous work have comprehensively studied on MWCNTs produced from waste tyres.[6-7, 11, 26] The preliminary investigations concerned different metal catalysts (Ni/Al$_2$O$_3$,Co/Al$_2$O$_3$/ Fe/Al$_2$O$_3$ and Cu/Al$_2$O$_3$), which were aiming to investigate the effects on both CNT and hydrogen productions by pyrolysis-catalysis of waste truck tyres. The results showed Ni/Al$_2$O$_3$ catalyst gave the highest hydrogen production at 18.14 mmol g^{-1}_{tyre} along with the production of relatively high-quality CNTs which were homogenous.[7] The influence of catalyst support was also investigated with different SiO$_2$:Al$_2$O$_3$ ratios (3:5, 1:1, 3:2, 2:1) with nickel. The results

showed that the Ni-based $SiO_2:Al_2O_3$ supported catalyst at a 1:1 ratio at 900 °C with tyre-to-catalyst ratios at 1:2 gave the highest hydrogen production of 27.41 mmol g^{-1}, and the 1:1 ratio gave the highest filamentous carbon production at 201.5 mg g^{-1}.[27] The influence of process parameters on hydrogen and CNT productions were investigated with the Ni/Al_2O_3 catalyst. Hydrogen production reached the highest level of 27.41 mmol g^{-1} at 900 °C with a sample-to-catalyst ratio of 1:2. The highest filamentous carbon production was obtained with tyre-to-catalyst ratio of 1:1 at 900 °C. The influence of water injection rate was also investigate that water introduction inhibited filamentous carbon production but increased hydrogen production.[6]

Three different tyre rubbers were investigated to study the mechanism of CNT formation from waste polymer.[8, 26] The results showed the natural rubber as the main component of most commercial tyres which isdominated to hydrogen production and styrene butadiene rubber gave the highest carbon formation. Due to the challenging process to purify CNT production, a nickel-basedcatalyst was loaded on stainless steel mesh and inttoduced in the plastic pyrolysis-catalysis investigation. The advantage of this catalyst showed that the formation of CNT could be easily removed by physical method from the mesh catalyst.[11] Fe-Ni bimetallic catalysts supported on MCM-41 with different Fe:Ni ratios were also studied with simulated mixed waste plastics. A synergistic effect of the iron and nickel was observed, particularly for the catalyst with Fe to Ni ratio at 10:10, where the highest gas yield (95 wt.%) and highest H_2 production (46.1 mmol $g^{-1}_{plastic}$) have been achieved. Along with lowest carbon deposition.[28]

We have recently published a review to highlight the future work regard the thermo-chemical conversion of carbonaceous waste for CNT and hydrogen productions, including the urged need to study CNT growth mechanism from waste materials. The existing mechanism is based on the model established decades ago using pure carbon precursors by CVD method. However, the mechanism of CNTs growth from waste carbonaceous materials is far more complicated as the waste precursor is extremely complex in terms of the composition and reactors are different as well. So, there is a need to carry out an in-depth study to understand the mechanism of CNT formation from waste materials in a specific reactor.[29]

This wide ranging suite of hydrocarbons will interact with the catalyst during the two-stage pyrolysis-catalysis process and produce carbon nano-materials. However, the influences of different tyre oil model compound on final carbon nano-material production has not been fully understood yet. In order to better understand the relative influences of the different chemical class fractions of tyre pyrolysis vapours/gases on carbon nano-material production, this work focus on the influence of tyre pyrolysis oil model compounds for production of carbon nano-materials. The model compounds consisted of two representative aliphatic compounds

(decane and hexadecane), one single ring aromatic hydrocarbon (styrene) and two polycyclic aromatic hydrocarbons (PAHs) (naphthalene and phenanthrene). The catalyst used was a 10 wt.% Ni/Al_2O_3 catalyst. The characteristics of the carbons produced from the model compounds was compared with the carbons produced from the pyrolysis-catalysis of waste truck tyres.

Materials and Methods

Materials

All model compounds used in this research were purchased from Sigma-Aldrich, UK. In addition, commercial carbon nano-filaments and MWCNTs were purchased from Sigma-Aldrich UK, to compare the characteristics of the carbon nano-materials produced from pyrolysis-catalysis process. The waste truck tyre was used as tyre rubber with the metal and fabric reinforcement removed and shredded to a particle size of ~ 6mm. For CHNS/O determination, an autosampler is connected to a quartz tube placed in a furnace at the temperature of 900 °C. This reactor is connected to the analytical column, which is connected to a channel of the thermal conductivity detector (TCD). The elemental analysis of the tyre showed a content of 81.16 wt.% carbon, 7.2 wt.% hydrogen, 0.8 wt.% nitrogen, ~8.74 wt.% (calculated by difference) and 2.1 wt.% sulphur.

The Ni/Al_2O_3 catalyst was prepared by an incipient wetness method with 10 wt.% nickel loading and alumina support. The procedure consisted of nickel nitrates were firstly dissolved in ethanol; alpha alumina powder was mixed with the nickel nitrate/ethanol solution with continuous stirring to produce a slurry. The slurry was dried overnight at 50 °C to evaporate the excess ethanol; the dried catalyst precursor was calcined for 3 hours at 750 °C in an air atmosphere. The catalyst was ground and sieved to a size range of 0.05 and 0.18 µm, and the catalyst was reduced *in-situ*.

Experimental system

The model compounds and truck tyre were reacted using the same two-stage pyrolysis-catalytic reactor used in previous work and a schematic diagram is shown in Figure 1. The reactors were constructed of stainless steel and were separately externally heated and controlled using electrical furnaces. Each model compound was placed in a sample crucible within the pyrolysis reactor. Exactly 0.5 g of the 10 wt.% Ni/Al_2O_3 catalyst was placed in the catalysis stage which was then pre-heated to the temperature of 800 °C and the pyrolysis stage was heated to 100 °C above the boiling point of each model compound at a heating rate of 40 °C min⁻¹. The weight of each type of model compound added to the first stage was calculated based on the carbon content of each gram of a typical waste truck tyre (81.16 wt.%

carbon content per gram of waste truck tyre).[7] Therefore, the weight of each model compound had the same amount of carbon content of 0.8116 g. The carbon:catalyst ratios were consistent with the carbon:catalyst ratio of 1.0 g of tyre sample to 0.5 g of catalyst which was 0.8116:0.5. Therefore, according to the molecular mass of the model compounds, 0.9572 g of hexadecane, 0.9624 g decane, 1.00 g styrene, 0.8668 naphthalene and 0.8610 phenanthrene were introduced in the experiments with 0.5 g of the 10 wt.% Ni/Al_2O_3 catalyst. The volatilised model compounds passed into the second stage reactor where they interacted with the catalyst at 800 °C. When truck tyre was investigated, exactly 1.0 g of the waste tyre rubber was placed in the sample crucible in the top pyrolysis reactor. Nitrogen was introduced from the top of the reactor at flow rate of 80 mL min^{-1}.
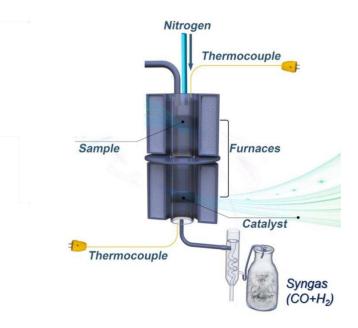

Figure 1 Schematic diagram of the two-stage fixed-bed reactor.

The product gases passed through a three-stage condensation system and were collected in a 25 L Tedlar^{TM} gas sample bag for gas chromatography (GC) analysis. The condensable products were collected in the condensers which were cooled by dry ice. The carbon production was obtained by weighting the reactor tube before and after the reaction. After each experiment the catalyst was cooled under nitrogen and removed from the reactor and stored for later analysis.

Analytical methods

The product gases were analysed for permanent gas (H_2, CO, O2 and N_2) content and hydrocarbon (C_2-C_4) content using two separate Varian 3380 GC gas chromatographs. The details of the columns used and analytical conditions have been reported previously.[6-9, 11, 27-28]

5

The deposits of carbon on the Ni/Al_2O_3 catalyst consist of a range of different carbon types, which may include, amorphous carbon, carbon nano-filaments and CNTs. The catalysts were therefore analysed by TPO which aid the identification of the different types of carbon deposited on the catalyst. The thermogravimetric analyser used was a Shimadzu TGA and the TPO process involves oxidation of the deposited carbon under controlled increase in temperature. The analysis was carried out with ~4 mg of reacted catalysts which was heated up to 850 °C at a controlled heating rate of 15 °C min^{-1} in an air atmosphere.

The surface morphology of the reacted catalysts with deposited carbon was determined by scanning electron microscopy (SEM) and transmission electron microscopy (TEM) using a Hitachi SU8230 scanning electron microscope and a FEI Tecnai TF20 transmission electron microscope. In addition, a Renishaw Invia Raman spectroscope to identify the degree of graphitization of different carbons produced from the different tyre oil model compounds by pyrolysis-catalysis. Analytical conditions used were, a wavelength of 514 nm at Raman shifts in the range of 100 to 3200 cm^{-1}.

Temperature programmed reduction (TPR) analysis has been carried out for the fresh catalysts with a Stanton-Redcroft thermo gravimetric analyser (TGA). Approximately 4 mg of the catalyst was preheated to 150 °C at a heating rate is 20 °C min^{-1} and held for 30 min in an atmosphere of mixed hydrogen and nitrogen, which consist of 5 vol.% H_2 and 95 vol.% N_2. The flow rate was 50 ml min^{-1}. Then, the sample was heated to 900 °C at a heating rate of 10 °C min^{-1}.

The fresh catalyst was also characterized by X-ray diffraction (XRD) on a Bruker D8 to identify the composition of the catalyst. The diffractometer used a Cu-Ka X-ray source with a Vantec position sensitive detector. The peaks at different diffraction angles in the spectra indicate the metal oxides sites which was identified by Pan Analytical Xpert High Score plus software. The sample preparation includes placing each of powdered samples on the pan before the start of the analysis. The analysis range (2 theta) was 10 to 70° with a scanning step of 0.05°. The entire analysis for each sample was around 30 mins which depended on the 2 theta and scanning step settings.

Fresh catalyst characterizations

Temperature programmed reduction (TPR) analysis for the fresh Ni/Al_2O_3 catalyst is shown in Figure 2 (a). There are two main reduction peaks at temperatures of ~230 and 800 °C which are assigned to the reduction of bulk NiO particles and Ni-Al spinel phases ($NiAl_2O_4$), respectively. The NiO and $NiAl_2O_4$ phases were also reported by Wu et al. [30] and Clause et al.[31] SEM micrograph of the fresh catalyst in Figure 2(b) shows that the surface structures of

the catalyst are composed of many irregular particles. $NiAl_2O_4$ and NiO phases were confirmed further confirmed by XRD in Figure 2(c) which will be reduced to Ni during the pyrolysis-catalysis process.
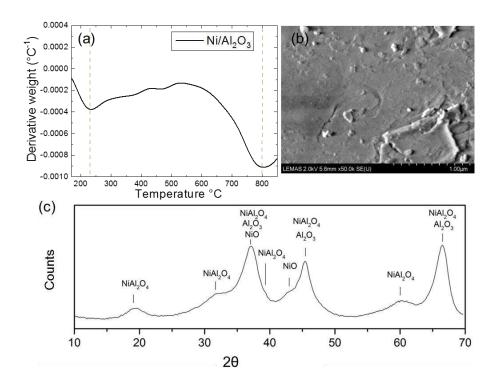

Figure 2 (a) Temperature programmed reduction (TPR) analysis; (b) SEM micrograph [Reprinted (adapted) with permission from {[7]}. Copyright {2015} American Chemical Society.] and (c) XRD of the fresh 10 wt.% Ni/Al_2O_3 catalyst.

Results and Discussion

Carbon production and characterisations

Table 1 shows the amount of carbon formed from the pyrolysis-catalysis of the tyre pyrolysis oil model compounds and truck tyre using the two-stage pyrolysis-catalysis reactor system with the 10% wt. Ni/Al_2O_3 catalyst. Table 1 shows that the aromatic and polycyclic aromatic model compounds produced higher carbon formation e.g. for styrene 0.4 g g^{-1} of feedstock equivalent carbon was produced, naphthalene produced 0.28 g g^{-1} of feedstock equivalent carbon and phenanthrene produced 0.29 g g^{-1} of feedstock equivalent carbon. This carbon formation was significantly higher than that produced from the aliphatic hydrocarbon model compounds from hexadecane and decane which were 0.06 and 0.2 g g^{-1} of feedstock equivalent carbon, respectively. Pyrolysis-catalysis of the truck tyre produced a carbon yield of 0.07 g g^{-1} of feedstock equivalent carbon which was significantly lower that the amount of carbon produced from the aromatic hydrocarbon model compounds.

Table 1 also illustrates the product gas composition from the pyrolysis-catalysis of the five tyre oil model compounds and from truck tyre. The gases produced include hydrogen, methane and C_2-C_4 hydrocarbons. The results show that the aliphatic model compounds (hexadecane and decane) are in favour of higher gaseous carbon production represented by CH_4 and C_2-C_4 hydrocarbons compared with the aromatic model compounds. Hexadecane produced 31.7 vol.% of CH_4 and 32.1 vol.% of C_2-C_4 hydrocarbons and decane produced 25.8 vol.% of CH_4 and 28.8 vol.% of C_2-C_4 hydrocarbons. These carbon containing gas concentrations were significantly higher than those produced with the aromatic compounds, styrene, naphthalene and phenanthrene. None of the C_2-C_4 hydrocarbons were found with phenanthrene. The results suggest that the molecular structures of the different model compounds influenced the gas composition produced from the pyrolysis-catalysis process. The straight chain aliphatic model compounds hexadecane and decane were easy to break down to lighter hydrocarbons corresponding with high gaseous carbon. The gas composition produced from the processing of the truck tyre produced CO, in addition to H_2, CH_4 and C_2-C_4 hydrocarbons.

Table 1 Carbon yield and gas composition for pyrolysis-catalysis of tyre pyrolysis oil model compounds and truck tyre.

	Hexadecane $C_{16}H_{34}$	Decane $C_{10}H_{22}$	Styrene C_8H_8	Naphthalene $C_{10}H_8$	Phenanthrene $C_{14}H_{10}$	Truck tyre
Carbon production*	0.06	0.20	0.40	0.28	0.29	0.07
Gas concentration (vol.%)						
H_2	36.2	45.5	86.3	93.9	98.1	49.6
CH_4	31.7	25.8	7.8	1.9	1.9	23.4
CO	-	-	-	-	-	19.4
C_2 - C_4 hydrocarbons	32.1	28.8	5.9	4.3	0.0	5.9

(*The unit for carbon production is g g^{-1} of feedstock equivalent carbon).

Temperature programmed oxidation of the reacted catalysts

Figure 3 shows the TPO of carbon deposited on the 10 wt. % Ni/Al$_2$O$_3$ catalysts from the pyrolysis-catalysis of the tyre pyrolysis oil model compounds. Figure 3(a) shows the weight loss data and Figure 3(b) shows the derivative or rate of weight loss data. The TPO analysis aims to compare the thermal stability of the different types of carbon deposited on the catalyst. Carbon oxidized below 600 °C has been assigned to the decomposition of amorphous carbon and the carbon oxidized above 600 °C has been assigned to the oxidation of filamentous type carbons [7]. The weight loss in Figure 3(a) and (b) indicate that the oxidation of carbon produced from different model compounds are in the temperature range of 450 to 750 °C. The TPO results indicate that the carbon formed consists of disordered/amorphous type carbons which

oxidize at lower temperature compared to graphitic/filamentous carbon which oxidize at higher temperature. The carbon with a high degree of graphitization would have a high thermal stability and would decompose at higher temperatures compared with the less graphitized/amorphous carbon.[32]
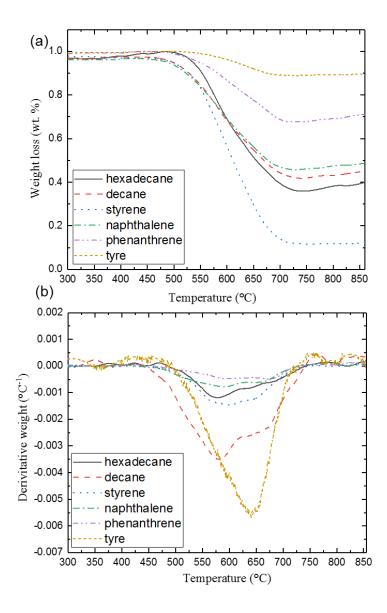

Figure 3 TGA-TPO results of reacted catalysts produced from pyrolysis-catalysis of tyre pyrolysis oil model compounds, (a) weight loss in relation to temperature, (b) derivative weight loss.

Based on the weight loss from the TPO results, the amount of amorphous and filamentous carbon production can be estimated. The proportions of amorphous and filamentous carbon produced from the different tyre pyrolysis oil model compounds and truck tyre are shown in

Figure 4. The figure shows that the aromatic and polycyclic aromatic hydrocarbons are dominant for solid carbon formation compared with the aliphatic model compounds and also for filamentous carbon formation. The filamentous carbon produced from styrene, naphthalene and phenanthrene were 174, 105 and 149 mg g^{-1} of feedstock equivalent carbon, respectively. Figure 4 shows that the amount of filamentous type carbon formed on the catalyst with styrene was 39.0% of the total carbon deposited, for naphthalene it was 37.3% and for phenanthrene it was 51.4% of the total carbon deposited. Comparison may be made with the carbon deposition on the catalyst for the aliphatic hydrocarbon model compounds. The filamentous carbon produced from the hexadecane and decane, aliphatic hydrocarbons which produced 27 and 78 mg g^{-1} of feedstock equivalent carbon, respectively. The amount of filamentous carbon for the hexadecane represented 45.1% of the total carbon deposited and for decane represented 39.0% of the total carbon. Comparison can be made with the amount of filamentous carbon produced from pyrolysis-catalysis of the truck tyre where the amount of filamentous carbon produced was 44 mg g^{-1} of feedstock equivalent carbon which represented 54% of the total carbon on the catalyst. A truck tyre may be composed of several different rubber elastomers such as natural rubber, polybutadiene rubber, nitrile rubber, styrene-butadiene rubber etc. Also, there is a significant proportion of carbon black which is used to strengthen the rubber and increase resistance to abrasion, and can comprise more than 20 wt.% of the tyre. All of these factors can influence the amount and type of carbon produced.
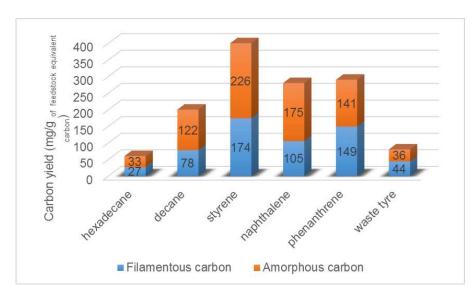

Figure 4 Proportions of disordered and filamentous types of carbon formed from the pyrolysis-catalysis of tyre oil model compounds and truck tyre.

 shows the SEM micrographs of the reacted 10 wt.% Ni/Al_2O_3 catalysts obtained from the pyrolysis-catalysis of the five tyre pyrolysis oil model compounds and the truck tyre. The

filamentous carbon formation from the different types of tyre pyrolysis oil model compounds are clearly illustrated in SEM images as shown in

.

Figure 5 SEM images of reacted catalysts produced from the pyrolysis-catalysis of (a)-(e) tyre oil model compounds and (f) truck tyre.

The SEM micrographs support the results obtained from TPO suggesting significant formation of filamentous carbons. The corresponding TEM images of the carbon formed on the catalyst with the model compounds are shown in Figure 6. The TEM images show that decane, styrene, naphthalene and phenanthrene produced MWCNTs with long tube length and smooth walls. Kumar and Ando[33-34] reported that the molecular structure of the precursors used for the production of CNTs by CVD directly affected the morphology of the growth of CNTs. Linear hydrocarbons such as methane, ethylene, and acetylene, produce hollow CNTs since the linear hydrocarbons are thermally decomposed into atomic carbons or linear dimer or trimer carbon. Characterisation of carbon deposits on the 10 wt.% Ni/Al_2O_3 catalyst from the pyrolysis-catalysis of truck tyre showed an entangled string-like filament structure similar to

that found with hexadecane, decane and styrene. TEM characterisation of the filaments found with the truck tyre showed that they consisted of both solid filaments and CNTs. Also the CNTs produced from truck tyre as shown in Figure 5 (f) and Figure 6 (f) are showing similarity to the commercial MWCNTs as shown in Figure 8 (c) and (d).

Cyclic hydrocarbons (such as benzene, xylene, cyclohexane, and fullerene) produce more curved CNTs.[34-36] The authors also reported that the relatively low temperature in the range of 600 to 900 °C is generally favored for MWCNTs production and single-walled CNTs (SWCNTs) are formed at higher temperature between 900 to 1200 °C by CVD. This could explain why no SWCNTs could be detected on the catalysts used in the pyrolysis-catalysis of tyre oil model compounds. If the SWCNTs appear in the carbon materials, there would be a series of bands appeared at the low frequency end of the spectrum known as Radial Breathing Mode (RBM). Chung and Jou[37-38]suggested that aliphatic olefins tend to produce long length CNTs during the pyrolysis of polyethylene and polypropylene in the presence of catalyst; whereas aromatic hydrocarbons facilitate the formation of CNTs with thicker walls through secondary pyrolytic deposition.

In addition, solid carbon nano-filaments could be observed in the carbons deposited on the catalyst for all of the aliphatic and aromatic hydrocarbons. Examples of solid nano-filaments formed from naphthalene are shown in the TEM images in Figure 6 (d) and for phenanthrene in (e). The formation of solid carbon nanofibers has been reported in the CNTs synthesis process by many researchers.[39-41] Mori and Suzuki[39] proposed that carbon nanofibers consist of several graphitic basal planes in carbon nanofibers synthesis by plasma-enhanced CVD. They reported that the carbon nanotubes consist of graphitic basal planes parallel to the fibre axis with a holey structure; or if the basal planes are perpendicular to the fiber axis this leads to a platelet structure of carbon nanofibers which are not hollow. Yoon et al.[40] also proposed a conceptual model to define the structures of carbon nanofibers synthesised by catalytic growth including the platelet type which indicates the formation of solid carbon nano-filaments, herringbone and tubular type carbon nano-filaments. The conceptual model has also been supported by Rodriguez et al.,[41] suggesting that the anisotropic alignment of graphene layers dominate carbon nano-filaments with diverse geometric structures, including platelet, herringbone and tubular carbon nano-filaments which all depend on the directions of alignment and filament axis.
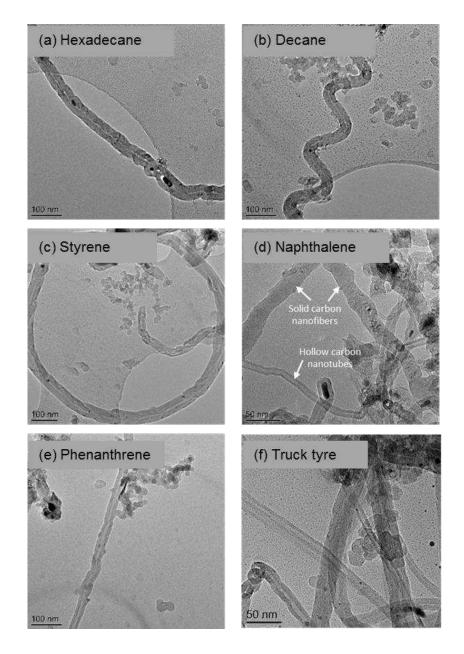
Figure 6 TEM images of reacted catalysts produced from the pyrolysis-catalysis of (a)-(e) tyre oil model compounds and (f) truck tyre.

The mechanism of carbon nano-filaments growth by catalytic decomposition of hydrocarbons has been studied by many researchers.[42-45] The possible routes include carbon precursor disassociation where the hydrocarbon molecules decompose on the free-metal surface and form carbon atoms. Alternatively, the mechanism involves hydrogen molecular desorption; diffusion of carbon atoms and nucleation whereby the carbon atoms precipitate as graphite on the metal surface.[44]The degree of crystallinity of the carbon nano-materials formed on the catalyst from the tyre pyrolysis oil model compounds and truck tyre during pyrolysis-catalysis can be characterised by Raman spectroscopy. The Raman spectra of the product carbons in the wavelength range of 500 to 3000 cm^{-1} are shown in Figure 7. Carbon is normally formed

as hybridizations including sp^1, sp^2 and sp^3, the different carbon allotropes either contain pure hybridizations or as a mixture. Carbon nanotubes, carbon nano-ribbons and amorphous carbon all contain different proportions of sp^2 and sp^3.[46] The D band evident at the Raman shift at 1300 cm^{-1} indicates disordered carbon or amorphous carbon (such as sp^3 bonding carbon or broken sp^2 bonding carbon). [47] The G band evident at 1550 cm^{-1} indicates the graphitized or filamentous structure of carbon (commonly for sp^2 carbon). The G' band occurred at wavelength 2700 cm^{-1} in the Raman shift indicates the defects in the graphitic crystallinity of carbon produced from the different model compounds which can be used to estimate the purity of carbon production.[6, 11] All sp^2 carbon materials have G' peaks in the Raman spectrum which is strongly dependent on the electronic and/or photon structure of graphene.

The intensity of the D band normalized to the intensity of the G band (I_D/I_G) can be used to determine the graphitization level of carbon. As Figure 7(a), (b) and (c) shows, the carbon produced from the polycyclic aromatic model compounds had relatively high I_D/I_G ratios, i.e. naphthalene and phenanthrene were 0.88 and 0.96, respectively. However, the carbons produced with aliphatic and single ring aromatic tyre oil model compounds had relatively low I_D/I_G ratios except of hexadecane was 0.87, the ratio for decane was 0.72 and styrene carbons had an ratio of 0.61. The ratios indicate the carbon produced from decane and styrene had a high degree of graphitization compared with the carbon produced from naphthalene and phenanthrene via the pyrolysis-catalysis process. Comparison of the Raman shift for the carbons produced from the pyrolysis-catalysis of truck tyre (Figure 7 (d)) showed I_D/I_G and $I_{G'}/I_G$ values of 0.78 and 0.43, respectively.
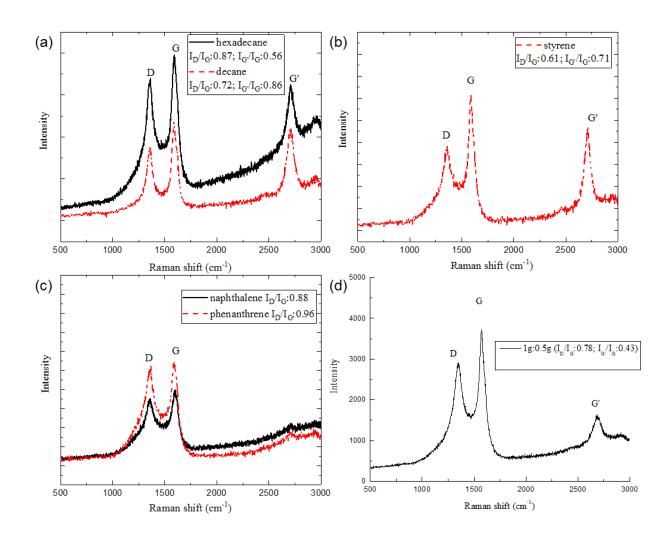
Figure 7 (a) Raman spectra of reacted catalysts produced from pyrolysis-catalysis of aliphatic tyre oil model compounds (hexadecane and decane); (b) single ring aromatic tyre oil model compounds (styrene); (c) polycyclic aromatic tyre oil model compounds (naphthalene and phenanthrene); (d) CNTs produced from truck tyre with track tyre-to-catalyst ratio at 1:0.5.

Figure 8 shows the Raman shift of commercial carbon nano-filaments and MWCNTs for comparison. The I_D/I_G ratio of carbon nano-filaments was 0.71 and the ratio of the commercial MWCNTs sample was also 0.71. This is in the range of the reported typical ratios of MWCNTs which is between 0.63-1.5.[48] The I_D/I_G ratios of carbon produced from the tyre pyrolysis oil model compounds are close to the ratios of commercial carbon nano-filaments and MWCNTs as shown in Figure 8. The data also indicates that the graphitization of the produced carbon is close to that of the commercially obtained samples.
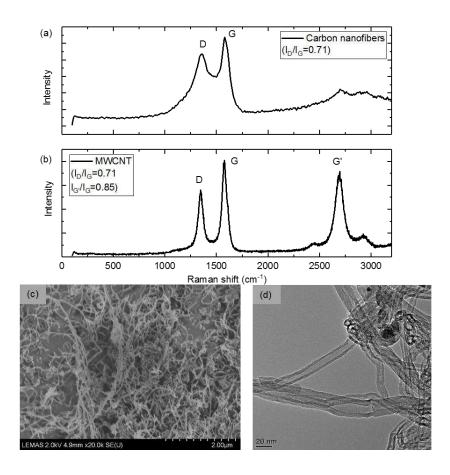
Figure 8 Raman spectra of commercial (a) carbon nanofibers and (b) MWCNTs; (c) SEM micrograph and (d) TEM micrograph of commercial MWCNTs.

The intensity of the G' band normalized to the intensity of the G band ($I_{G'}/I_G$) can be used to estimate the purity of the carbon produced. The $I_{G'}/I_G$ ratio of carbon produced from hexadecane had the lowest ratio at 0.56 which suggests that the carbon produced had more defects and low purity compared with the carbon produced from decane and styrene. This is because the G' band arises from the two-photon scattering elastic process which indicates the long-range order of the sample. The lower intensity of the G' band indicates the samples are less ordered, for example, containing a high amount of impurities thereby not allowing the coupling effect for the two-photon process.[43-44] The $I_{G'}/I_G$ ratios of carbon produced from decane and styrene were 0.86 and 0.71 which are close to the ratio of commercial MWCNTs at 0.85 as shown in Figure 8. The results also support the suggestion that the carbon produced from decane and styrene can achieve that of the commercial MWCNTs quality. Figure 7(d) and 6(e) shows that the carbon produced from naphthalene and phenanthrene have no significant G' peaks that are similar to the commercial carbon nano-filaments shown in Figure 8. The TEM images in Figure 6(d) and 6(e) confirms that there are carbon nano-filaments in addition to the MWCNTs.

Conclusions

This work is focused on the influence of the chemical structures of tyre pyrolysis oil model compounds on the formation of carbon nano-materials. The aliphatic model compounds (hexadecane and decane) favor gaseous hydrocarbon formation instead of solid carbon formation in the waste tyre pyrolysis-catalysis process. Hexadecane and decane with relatively high gaseous carbon conversion ratios compared with aromatic compounds which are 42.6 and 32.74 vol.%, respectively, corresponded with lower carbon formation which are 0.06 and 0.2 g g^{-1}_{of feedstock equivalent carbon}. Aromatic compounds (styrene, naphthalene and phenanthrene) dominate the production of solid carbon in a range of 0.28 to 0.4 g g^{-1}_{of feedstock equivalent carbon}, especially for filamentous carbon formation compared to the aliphatic compounds (hexadecane and decane). However, the chemical structure of decane with shorter linear structure compared with hexadecane favors a higher quantity of filamentous carbon formation that are mostly MWCNTs. The aromatic model compounds favor solid carbon formation where the majority of carbon formation is filamentous carbon including hollow CNTs and solid carbon nano-filaments which was confirmed by TEM micrographs and comparing with the commercial nano-carbon products. The polycyclic aromatic compounds produced more solid carbon nano-filaments compared to the single ring aromatic model compound. The single ring aromatic compound styrene produced the highest quantity of carbon and filamentous carbon which was 0.4 g g^{-1}_{of feedstock equivalent carbon} and 174 mg g^{-1}_{of feedstock equivalent carbon}, respectively.

Author Contributions: Conceptualization, Y.S.Z. and P.T.W.; methodology, Y.S.Z.; software, R.K.Z., Z.Q.L. and Y.S.Z.; validation, Y.S.Z. and P.T.W.; formal analysis, Y.S.Z.; investigation, Y.S.Z. and H.L.Z.; resources, P.T.W.; data curation, Y.S.Z., R.K.Z. and H.L.Z.; writing-original draft preparation, Y.S.Z.; writing, H.L.Z., R.K.Z. and L.Y.; visualization, H.L.Z., Z.Q.L. and R.K.Z.; supervision, P.T.W.; project administration, Y.S.Z.; funding acquisition, Y.S.Z. and R.K.Z. All authors have read and agreed to the published version of the manuscript

Conflicts of Interest: The authors declare no conflict of interest.

References

(1) Iijima, S. Helical microtubules of graphitic carbon. *nature* **1991,** *354* (6348), 56-58.
(2) Chen, D.; Christensen, K. O.; Ochoa-Fernández, E.; Yu, Z.; Tøtdal, B.; Latorre, N.; Monzón, A.; Holmen, A. Synthesis of carbon nanofibers: effects of Ni crystal size during methane decomposition. *Journal of Catalysis* **2005,** *229* (1), 82-96.

(3) Takenaka, S.; Ishida, M.; Serizawa, M.; Tanabe, E.; Otsuka, K. Formation of carbon nanofibers and carbon nanotubes through methane decomposition over supported cobalt catalysts. *The Journal of Physical Chemistry B* **2004,** *108* (31), 11464-11472.

(4) Meshot, E. R.; Plata, D. L.; Tawfick, S.; Zhang, Y.; Verploegen, E. A.; Hart, A. J. Engineering vertically aligned carbon nanotube growth by decoupled thermal treatment of precursor and catalyst. *Acs Nano* **2009,** *3* (9), 2477-2486.

(5) Wang, G.; Wang, H.; Tang, Z.; Li, W.; Bai, J. Simultaneous production of hydrogen and multi-walled carbon nanotubes by ethanol decomposition over Ni/Al2O3 catalysts. *Applied Catalysis B: Environmental* **2009,** *88* (1-2), 142-151.

(6) Zhang, Y.; Williams, P. T. Carbon nanotubes and hydrogen production from the pyrolysis catalysis or catalytic-steam reforming of waste tyres. *Journal of Analytical and Applied Pyrolysis* **2016,** *122*, 490-501.

(7) Zhang, Y.; Wu, C.; Nahil, M. A.; Williams, P. Pyrolysis–Catalytic Reforming/Gasification of Waste Tires for Production of Carbon Nanotubes and Hydrogen. *Energy & Fuels* **2015,** *29* (5), 3328-3334.

(8) Zhang, Y.; Wu, C.; Nahil, M. A.; Williams, P. High-value resource recovery products from waste tyres. *Proceedings of the Institution of Civil Engineers–Waste and Resource Management* **2016,** *169* (3), 137-145.

(9) Zhang Yeshui, T. Y., Huang Jun, Williams Paul. Influence of silica-alumina supports on H2 and Carbon Nanotube production during the catalytic pyrolysis of waste tyres on Ni catalysts. *Waste management & research* **2016,** *35* (10), 1045-1054.

(10) Gong, J.; Liu, J.; Jiang, Z.; Chen, X.; Wen, X.; Mijowska, E.; Tang, T. Converting mixed plastics into mesoporous hollow carbon spheres with controllable diameter. *Applied Catalysis B: Environmental* **2014,** *152*, 289-299.

(11) Zhang, Y.; Nahil, M. A.; Wu, C.; Williams, P. T. Pyrolysis–catalysis of waste plastic using a nickel–stainless-steel mesh catalyst for high-value carbon products. *Environmental technology* **2017,** *38* (1), 1-9.

(12) Yao, D.; Zhang, Y.; Williams, P. T.; Yang, H.; Chen, H. Co-production of hydrogen and carbon nanotubes from real-world waste plastics: Influence of catalyst composition and operational parameters. *Applied Catalysis B: Environmental* **2018,** *221*, 584-597.

(13) Wu, C.; Wang, Z.; Williams, P. T.; Huang, J. Renewable hydrogen and carbon nanotubes from biodiesel waste glycerol. *Scientific reports* **2013,** *3*.

(14) Zhang, S.; Jiang, S.-F.; Huang, B.-C.; Shen, X.-C.; Chen, W.-J.; Zhou, T.-P.; Cheng, H.-Y.; Cheng, B.-H.; Wu, C.-Z.; Li, W.-W.; Jiang, H.; Yu, H.-Q. Sustainable production of value-added carbon nanomaterials from biomass pyrolysis. *Nature Sustainability* **2020**, DOI: 10.1038/s41893-020-0538-1.

(15) He, L.; Hu, S.; Jiang, L.; Liao, G.; Zhang, L.; Han, H.; Chen, X.; Wang, Y.; Xu, K.; Su, S.; Xiang, J. Co-production of hydrogen and carbon nanotubes from the decomposition/reforming of biomass-derived organics over Ni/α-Al2O3 catalyst: Performance of different compounds. *Fuel* **2017,** *210*, 307-314, DOI: 10.1016/j.fuel.2017.08.080.

(16) Arabiourrutia, M.; Lopez, G.; Artetxe, M.; Alvarez, J.; Bilbao, J.; Olazar, M. Waste tyre valorization by catalytic pyrolysis–A review. *Renewable and Sustainable Energy Reviews* **2020,** *129*, 109932.

(17) Elbaba, I. F.; Williams, P. T. Deactivation of Nickel Catalysts by Sulfur and Carbon for the Pyrolysis–Catalytic Gasification/Reforming of Waste Tires for Hydrogen Production. *Energy & Fuels* **2014,** *28* (3), 2104-2113, DOI: 10.1021/ef4023477.

(18) Elbaba, I. F.; Williams, P. T. Two stage pyrolysis-catalytic gasification of waste tyres: Influence of process parameters. *Applied Catalysis B: Environmental* **2012,** *125* (0), 136-143.

(19) Elbaba, I. F.; Williams, P. T. High yield hydrogen from the pyrolysis–catalytic gasification of waste tyres with a nickel/dolomite catalyst. *Fuel* **2013,** *106* (0), 528-536.

(20) Elbaba, I. F.; Wu, C.; Williams, P. T. Catalytic Pyrolysis-Gasification of Waste Tire and Tire Elastomers for Hydrogen Production. *Energy & Fuels* **2010,** *24* (7), 3928-3935, DOI: 10.1021/ef100317b.

(21) Elbaba, I. F.; Wu, C.; Williams, P. T. Hydrogen production from the pyrolysis–gasification of waste tyres with a nickel/cerium catalyst. *International Journal of Hydrogen Energy* **2011,** *36* (11), 6628-6637.

(22) Yang, W.; Sun, W. J.; Chu, W.; Jiang, C. F.; Wen, J. Synthesis of carbon nanotubes using scrap tyre rubber as carbon source. *Chinese Chemical Letters* **2012,** *23* (3), 363-366.

(23) Murr, L. E.; Brown, D. K.; Esquivel, E. V.; Ponda, T. D.; Martinez, F.; Virgen, A. Carbon nanotubes and other fullerenes produced from tire powder injected into an electric arc. *Materials Characterization* **2005,** *55* (4), 371-377.

(24) Poyraz, S.; Liu, Z.; Liu, Y.; Zhang, X. Devulcanization of scrap ground tire rubber and successive carbon nanotube growth by microwave irradiation. *Current Organic Chemistry* **2013,** *17* (20), 2243-2248.

(25) Williams, P. T. Pyrolysis of waste tyres: a review. *Waste management* **2013,** *33* (8), 1714-1728.

(26) Zhang, Y. Hydrogen and carbon nano-materials from the pyrolysis-catalysis of wastes. University of Leeds, 2017.

(27) Zhang, Y.; Tao, Y.; Huang, J.; Williams, P. Influence of silica–alumina support ratio on H2 production and catalyst carbon deposition from the Ni-catalytic pyrolysis/reforming of waste tyres. *Waste Management & Research* **2017,** *35* (10), 1045-1054.

(28) Zhang, Y.; Huang, J.; Williams, P. T. Fe–Ni–MCM-41 Catalysts for Hydrogen-Rich Syngas Production from Waste Plastics by Pyrolysis–Catalytic Steam Reforming. *Energy & Fuels* **2017,** *31* (8), 8497-8504, DOI: 10.1021/acs.energyfuels.7b01368.

(29) Zhang, Y.; Zhu, H.; Yao, D.; Williams, P. T.; Wu, C.; Xu, D.; Hu, Q.; Manos, G.; Yu, L.; Zhao, M. Thermo-chemical conversion of carbonaceous waste for CNT and hydrogen productions: A review. *Sustainable Energy & Fuels* **2021**.

(30) Wu, C.; Williams, P. T. Investigation of Ni-Al, Ni-Mg-Al and Ni-Cu-Al catalyst for hydrogen production from pyrolysis–gasification of polypropylene. *Applied Catalysis B: Environmental* **2009,** *90* (1–2), 147-156.

(31) Clause, O.; Gazzano, M.; Trifiro′, F.; Vaccari, A.; Zatorski, L. Preparation and thermal reactivity of nickel/chromium and nickel/aluminium hydrotalcite-type precursors. *Applied Catalysis* **1991,** *73* (2), 217-236.

(32) Kukovitskii, E.; Chernozatonskii, L.; L'vov, S.; Mel'Nik, N. Carbon nanotubes of polyethylene. *Chemical physics letters* **1997,** *266* (3-4), 323-328.

(33) Kumar, M.; Ando, Y. Controlling the diameter distribution of carbon nanotubes grown from camphor on a zeolite support. *Carbon* **2005,** *43* (3), 533-540

(34) Kumar, M.; Ando, Y. Chemical vapor deposition of carbon nanotubes: a review on growth mechanism and mass production. *Journal of nanoscience and nanotechnology* **2010,** *10* (6), 3739-3758.

(35) Morjan, R. E.; Nerushev, O. A.; Sveningsson, M.; Rohmund, F.; Falk, L. K. L.; Campbell, E. E. B. Growth of carbon nanotubes from C60. *Applied Physics A* **2004,** *78* (3), 253-261, DOI: 10.1007/s00339-003-2297-z.

(36) Nerushev, O. A.; Dittmar, S.; Morjan, R.-E.; Rohmund, F.; Campbell, E. E. B. Particle size dependence and model for iron-catalyzed growth of carbon nanotubes by thermal chemical vapor deposition. *Journal of Applied Physics* **2003,** *93* (7), 4185-4190.

(37) Chung, Y.-H.; Jou, S. Carbon nanotubes from catalytic pyrolysis of polypropylene. *Materials chemistry and physics* **2005,** *92* (1), 256-259.

(38) Wu, C.; Wang, Z.; Williams, P. T.; Huang, J. Renewable hydrogen and carbon nanotubes from biodiesel waste glycerol. *Scientific Reports* **2013,** *3*, 1-6.

(39) Mori, S.; Suzuki, M. *Non-Catalytic, Low-Temperature Synthesis of Carbon Nanofibers by Plasma-Enhanced Chemical Vapor Deposition*, 2010.

(40) Yoon, S.-H.; Lim, S.; Hong, S.-h.; Qiao, W.; Whitehurst, D. D.; Mochida, I.; An, B.; Yokogawa, K. A conceptual model for the structure of catalytically grown carbon nano-fibers. *Carbon* **2005,** *43* (9), 1828-1838.

(41) Rodriguez, N. M.; Chambers, A.; Baker, R. T. K. Catalytic engineering of carbon nanostructures. *Langmuir* **1995,** *11* (10), 3862-3866.

(42) Oberlin, A.; Endo, M.; Koyama, T. Filamentous growth of carbon through benzene decomposition. *Journal of crystal growth* **1976,** *32* (3), 335-349.

(43) Yang, R.; Chen, J. Mechanism of carbon filament growth on metal catalysts. *Journal of Catalysis* **1989,** *115* (1), 52-64.

(44) De Jong, K. P.; Geus, J. W. Carbon Nanofibers: Catalytic Synthesis and Applications. *Catalysis Reviews* **2000,** *42* (4), 481-510, DOI: 10.1081/CR-100101954.

(45) Jie, X.; Li, W.; Slocombe, D.; Gao, Y.; Banerjee, I.; Gonzalez-Cortes, S.; Yao, B.; AlMegren, H.; Alshihri, S.; Dilworth, J. Microwave-initiated catalytic deconstruction of plastic waste into hydrogen and high-value carbons. *Nature Catalysis* **2020**, 1-11.

(46) Somani, P. R.; Umeno, M. Importance of transmission electron microscopy for carbon nanomaterials research. *Modern Research and Educational Topics in Microscopy* **2007,** *3*, 634-42.

(47) DiLeo, R. A.; Landi, B. J.; Raffaelle, R. P. Purity assessment of multiwalled carbon nanotubes by Raman spectroscopy. *Journal of Applied Physics* **2007,** *101* (6), 064307.

(48) Wu, C.; Wang, Z.; Wang, L.; Williams, P. T.; Huang, J. Sustainable processing of waste plastics to produce high yield hydrogen-rich synthesis gas and high quality carbon nanotubes. *RSC Advances* **2012,** *2* (10), 4045-4047, DOI: 10.1039/c2ra20261a.